Insight on Tricalcium Silicate Hydration and Dissolution Mechanism from Molecular Simulations

Hegoi Manzano,[*,†] Engin Durgun,[‡] Iñigo López-Arbeloa,[†] and Jeffrey C. Grossman[§]

[†]Molecular Spectroscopy Laboratory, Physical Chemistry Department, University of the Basque Country, Barrio Sarriena s/n, Leioa, 48940 Bizkaia, Spain

[‡]UNAM-National Nanotechnology Research Center and Institute of Materials Science and Nanotechnology, Bilkent University, Ankara 06800, Turkey

[§]Department of Materials Science and Engineering, Massachusetts Institute of Technology, Cambridge, Massachusetts 02139, United States

S *Supporting Information*

ABSTRACT: Hydration of mineral surfaces, a critical process for many technological applications, encompasses multiple coupled chemical reactions and topological changes, challenging both experimental characterization and computational modeling. In this work, we used reactive force field simulations to understand the surface properties, hydration, and dissolution of a model mineral, tricalcium silicate. We show that the computed static quantities, i.e., surface energies and water adsorption energies, do not provide useful insight into predict mineral hydration because they do not account for major structural changes at the interface when dynamic effects are included. Upon hydration, hydrogen atoms from dissociated water molecules penetrate into the crystal, forming a disordered calcium silicate hydrate layer that is similar for most of the surfaces despite wide-ranging static properties. Furthermore, the dynamic picture of hydration reveals the hidden role of surface topology, which can lead to unexpected water tessellation that stabilizes the surface against dissolution.

KEYWORDS: dissolution, hydration, molecular dynamics, surface properties, water adsorption, calcium silicate
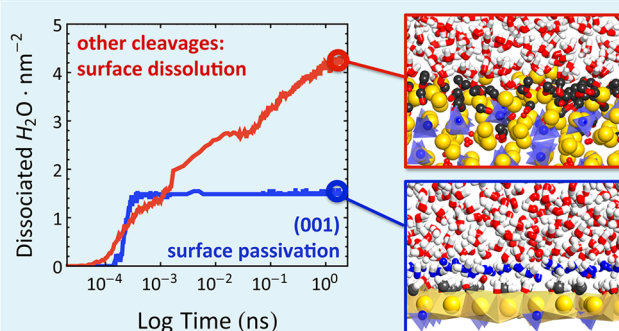
■ INTRODUCTION

The hydration and dissolution of minerals is of crucial importance for a broad range of natural and synthetic phenomena: from the stability of minerals and rocks in watersheds and aquifers,[1] to hydrogen production and other heterogeneous catalytic reactions,[2,3] to the production, utilization, and ultimate degradation of building materials,[4] and to the durability of biomaterials,[5] to name only a few examples. The key properties at play during dissolution are controlled by interfacial reactions between water molecules and the solid surfaces, which can be probed experimentally via techniques such as AFM, vertical scanning interferometry (VSI), and the study of isotope exchange or solute fluxes to provide general information regarding the reaction rates or qualitative information about the formation of steps, pitches, and so on.[6] However, in many applications, much more control over the hydration and dissolution is desired, such as the ability to moderate the rate[7] or preferentially favor the dissolution of one crystal facet over other.[8] To achieve such control, a deeper understanding of the molecular mechanisms governing hydration and dissolution is necessary.

In this work, we use atomic-scale simulations to study the hydration of a calcium orthosilicate. We take a multistep approach, which is critical to piece together the relevant physical processes underlying hydration and dissolution. First, we analyze the surface energies and water molecule adsorption, extending beyond traditional approaches in order to obtain a more accurate picture of these properties. Next, we compare these surface properties with the results obtained from simulating a realistic hydration process over a period of 2 ns. We discuss the differences between the static and dynamic pictures and show that topological changes render the properties of the former useless for predicting mineral hydration processes. A number of features related to the dissolution of the surface appear only in the context of accurate molecular dynamics simulations over relatively long time scales.[9,10] We have chosen tricalcium silicate as a model system because of its technological interest. (It is the most abundant phase in ordinary portland cement.) With more than 3×10^9
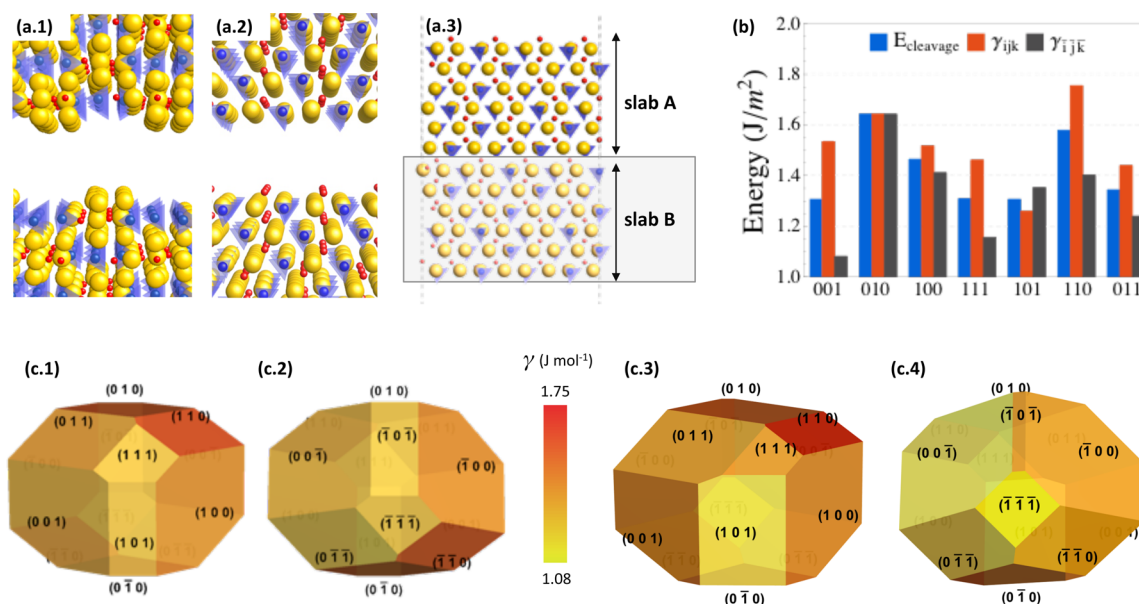
Figure 1. (a.1 and a.2) Representation of the surfaces originated by cleaving Ca$_3$SiO$_2$ through the symmetric (010) plane and the asymmetric (001) planes, respectively. For the asymmetric case (a.2), the independent surface energies can be obtained by dividing the system into two subslabs and computing their energies independently, as shown in a.3. The bottom surface of slab A is in contact with slab B, and it can effectively be considered to be in the bulk. (b) Computed surface and cleavage energies. The cleavage energy is calculated using the traditional definition of the surface energy,[26] whereas the individual surface energies are calculated using the split-slab method presented here. Two views of the Wulff shape constructed using (c.1 and c.2) cleavage energies and (c.3 and c.4) using the individual surface energies. The asymmetric equilibrium morphology can be observed in the latter.

tons of cement produced worldwide per year[11] and roughly 7.5 × 10^9 m^3 of water used to hydrate it (equivalent to 3 million Olympic-size swimming pools), the dissolution of this material represents arguably the most abundant and technologically relevant mineral hydration reaction, yet surprisingly little is known about the mechanism behind tricalcium silicate hydration, especially at short hydration times.[12]

COMPUTATIONAL METHODS

The simulations were carried out using the ReaxFF reactive force field[13] as implemented in the LAMMPS simulation package.[14] The ReaxFF set of parameters employed in this study was created merging the Si−O−H and Ca−O−H sets developed independently by Fogarty et al.[15] and Manzano et al.[16] The full set has been previously employed to study structural and mechanical properties of amorphous and crystalline calcium silicate hydrates[17−20] and clays.[21,22] A test on the accuracy of ReaxFF capturing water dissociation reaction in a calcium orthosilicate model cluster is included in the Supporting Information.

From bulk tricalcium silicate, we built slabs at least 4 nm thick and larger than 2.5 nm in the periodic directions. The vacuum region was set to 3 nm in all the cases. Energy minimizations were done using the Polak−Ribière version of the conjugate gradient algorithm, with cutoff tolerances of 10^{-5} kcal mol^{-1} and 10^{-6} kcal mol^{-1} A^{-1} for the energy and forces, respectively. Molecular dynamics were carried out in the canonical ensemble at 298 K and 1 atm, with a Nose−Hoover thermostat constant of 20 fs, integrating the equations of motions using the velocity−Verlet algorithm with a time step of 0.2 fs. For each slab, the appropriate number of water molecules to match a density of 1 g cm^{-3} in the vacuum region were placed randomly using packmol[23] and then relaxed independently from the slab. The water and the crystal surfaces were then put into contact and the dynamics started with initial random velocities generated from a Gaussian distribution of energies at 298 K. To avoid energy transfer to zero-frequency modes, the velocity of the center of masses was removed every 10^3 steps.

RESULTS AND DISCUSSION

Static Picture 1: Bare Surface Energetics. The disruption of the atomic structure via the formation of a surface, compared to the arrangement in the bulk, induces a free-energy defect referred to as the surface energy. High values of the surface energy indicate larger surface instabilities because of undercoordinated atoms and strained or broken bonds. It is reasonable to assume that for a given crystal less stable surfaces will tend to be more reactive and to develop stronger chemical interactions that lead to surface energy minimization.[24,25] Thus, we begin our analyses of the static picture with a set of calculations of the surface energies for low-index planes.

Surface energies (γ) are routinely computed from atomistic simulations using the relationship

$$\gamma = \frac{1}{2}\frac{G_{\text{slab}} - nG_{\text{bulk}}}{A} \tag{1}$$

where G_{slab} and G_{bulk} are the free energies of the constructed slab and the bulk material, respectively, n is the number of bulk units cell used to create the slab in the perpendicular direction, and A is the area of the generated surfaces. This expression assumes that the slab has the same termination in both sides, hence the factor $^1/_2$. In crystals with low symmetry, this assumption is not always fulfilled, and the surface energy is actually the cleavage energy, i.e., an average of the top and bottom surface energy values. Tricalcium silicate has a symmetry group of Cm, so we can construct symmetrically equivalent surfaces only in the (010) direction if a glide symmetry operation is applied.[27]

Various strategies have been used to overcome this problem in some specific cases. For instance, the energy of surfaces with steps and kinks can be computed if a symmetric slab is available as a reference.[28] In slabs with different composition in each side, the relative surface energies can be obtained as a function
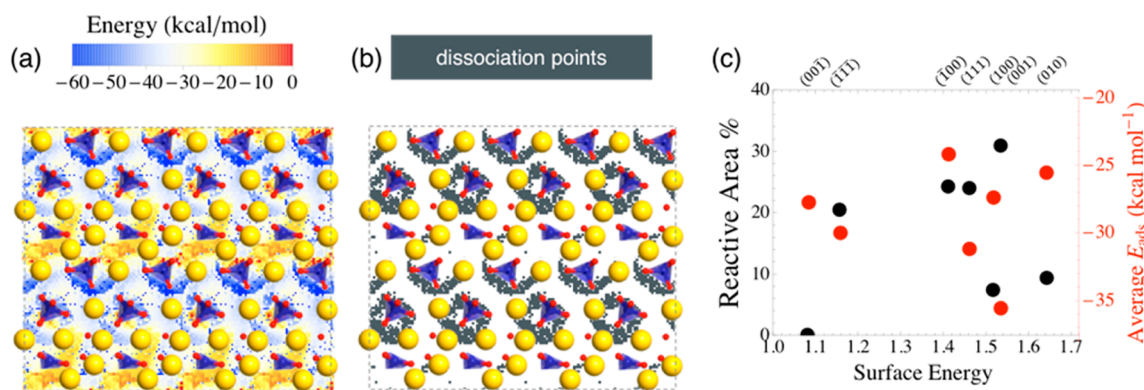
Figure 2. (a) Computed adsorption energy surface (AES) for the (111) surface. The color scale represents the adsorption energy of a water molecule in that given surface site. The higher adsorption energy areas (blue) could lead to dissociative sorption in some points, represented in b as dark pixels. The AES and dissociation sites for the remaining surfaces are presented in the Supporting Information. (c) Scatter plot of the relationship among the surface energy, the average water adsorption energy (red), and percentage of area where water dissociates (black). The lack of correlation between these properties is manifest.

of the chemical potential of the components.[29] Here we have used a new approach based on a split evaluation of the slab energy. We group the atoms in two equivalent subslabs A and B, as shown in Figure 1a. Slab A has one surface exposed to the vacuum, whereas the other is in contact with slab B, which is equivalent to being in the bulk if slab B slab is thick enough. In such a system, the energy difference between the bulk and subslab A comes only from a single surface contribution, and the surface energies can be computed as

$$\gamma = \frac{G_{\text{slab(A,B)}} - n_{\text{(A,B)}} G_{\text{bulk}}}{A} \qquad (2)$$

where all the quantities denote the same variables as in eq 1, except that n is the number of bulk units cell used to create the subslab in the perpendicular direction. Essentially, this approach is simply dividing the energy of slab into the contribution of two separate groups so that each surface is evaluated independently. This procedure can be used to evaluate independently the surface energy of asymmetric slabs or surfaces with structural imperfections without any other reference system than the bulk.

The computed surface energies are in the range of 1.08−1.75 J m^{-2}, in good agreement with more accurate quantum mechanical calculations[29] as well as empirical simulations.[30] As shown in Figure 1b, the decomposition into independent surface energies reveals a considerable difference between complementary surfaces, up to 25% of the maximum value. The importance of this difference cannot be understated. Note that both the maximum and minimum energy surfaces are incorrectly identified with the standard cleavage energy (average over both surfaces): One of the sides of the (110) cut is the highest energy surface as opposed to the (010) surface predicted by the average cleavage energy, whereas one of the sides of the (001) cut is the lowest energy case, the value of which is considerably lower than the lowest surface energy predicted by the average cleavage energy.

In addition to the importance of identifying the lowest energy facets, the combination of surface energies is crucial in order to predict realistic Wulff shapes and corresponding exposed facets in a particle. As can be seen in Figure 1c, crystal asymmetry has a strong impact on the equilibrium morphology, which is of great significance for the study and development of low-symmetry materials in a range of applications.[31]

Static Picture 2: Water Sorption Energetics. Beyond the bare surface energies, a static approach often employed to understand the propensity of mineral surfaces toward hydration involves the calculation of the water physi- or chemisorption energies.[32−34] The surfaces of tricalcium silicate are heterogeneous and present multiple possible adsorption sites where water molecules could physisorb and/or dissociate. To view the energetics of this landscape for the full surface (as opposed to simply the most stable adsorption site), we have constructed the adsorption energy surface (AES) of a water molecule over Ca_3SiO_2 surfaces. A water molecule is placed in a fine grid of positions near the surfaces, fixing the oxygen atom position in the plane parallel to the surface while allowing structural relaxation of both the surface and the molecule. To avoid artifacts caused by the initial water molecule alignment, 12 orientations were tested at each point of the grid. The most stable configuration and energy at each point are recorded, leading to a map of adsorption energies, i.e., the AES. In addition, we verify at each point of the computed AES whether the water molecule undergoes dissociation or not and construct the corresponding dissociation map. An example of the AES and dissociation map is shown in Figure 2. (The Supporting Information contains further details regarding the procedure to build them as well as the full results for all surfaces.)

The AES are considerably heterogeneous and differ from one surface to another because of the low symmetry of the crystal. There are multiple possible adsorption sites, but in general, the water oxygen atom is coordinated to a surface calcium cation and the hydrogen atoms tend to form hydrogen bonds with surface oxygen anions. In some cases, when the surface topology presents a cation−anion pair at an appropriate distance, the water molecule dissociates forming a hydroxyl pair, as found for alkaline earth oxides,[16,32] metallic oxides,[35,36] and binary oxides.[37,38] It is interesting to note that such dissociative adsorption can take place during energy minimization, indicating a reaction without energy barrier. Furthermore, the reaction can take place independently whether the ionic oxygen or silicate oxygen atoms are involved. DFT simulations[26,39] showed that in the bulk crystal the ionic oxygen atom is more reactive than the silicate one, yet that difference is apparently dismissed in the surface.

The most probable dissociative and associative configurations are detailed in the Supporting Information. Nevertheless, the

main advantage of the AES is that we can study the energetics of the adsorption globally, rather than at only a single (e.g., the most energetic) adsorption site. The average adsorption energy values range between −36 and −24 kcal mol^{-1}, corresponding to the (010) and (001) surfaces, respectively.

A fundamental step during hydration and dissolution is the reaction of water molecules with the solid surface. Therefore, the reactivity can be related to the amount of surface area where water undergoes chemisorption. As expected, the points where water reacts are those with the highest energy in the AES because dissociative sorption is generally more energetic than associative sorption. According to our simulations, the (001) surface has the largest reactive area, about 30% of the total, whereas its complementary (00$\bar{1}$) surface does not show any spontaneous reactive site.

As mentioned above, the relative surface energy for a crystal is usually proportional to the degree of undercoordination of the atoms at the surface.[27] However, our calculations noticeably show that there is no direct correlation between the surface energies of the crystalline slab and the surface area where water reacts or its average adsorption energy, as can be see in Figure 2c. A surface with a large number of undercoordinated cations might translate into a high surface energy, but if the anionic counterpart is not at an appropriate position, then (dissociative) adsorption might not be favorable. Hence, there is no necessary correlation between surface energies and the water adsorption energies because consideration of the distinct topological aspects of the surface is crucial in each case.

Dynamic Picture 1: Hydration and Early Dissolution Process. The static energetics of the interaction of water with the surface can provide important intuition regarding the zero-time picture. However, in order to understand the initial hydration mechanism of a tricalcium silicate surface, we allow time to evolve, following the dynamics of a system composed by tricalcium silicate slabs in contact with bulk water at room temperature and under pressure conditions for a period of 2 ns. In Figure 3a, we show the number of water molecules reacted per surface area for the different cleavages. There is an initial rapid step (∼0.3 ns) when water dissociates on the bare crystal surfaces, after which the hydration process enters a second stage when the reactions slow down and reach a steady-state regime. It is noteworthy that different surfaces, despite possessing quite different static energetics, reach the steady-state regime at roughly the same time in our simulations and that the number of water molecules dissociated per surface area is almost identical. (There is a clear exception for the (001) surface that we will discuss later in detail.)

According to our MD simulations, the hydration mechanism of tricalcium silicate can be described as a "reaction and hopping" process. First, water molecules dissociate in the surface to form hydroxyl pairs. Then, there is a proton hopping from the hydroxyl groups toward the inner oxygen atoms, leaving the initial oxygen atom free for posterior water dissociation (details in the Supporting Information). The same type of mechanism has been observed in the hydration of silica glasses.[15,40] However, we did not observe hydronium ions or pentacoordinated silicon during the proton hopping. These species facilitate proton transfer between bridging oxygen atoms within the rigid 3D network in silicate glasses.[40] In contrast, tricalcium silicate is more flexible because of the lack of a 3D covalent bond network,[39,41] which makes unnecessary the formation of hydronium ions. Protons can therefore
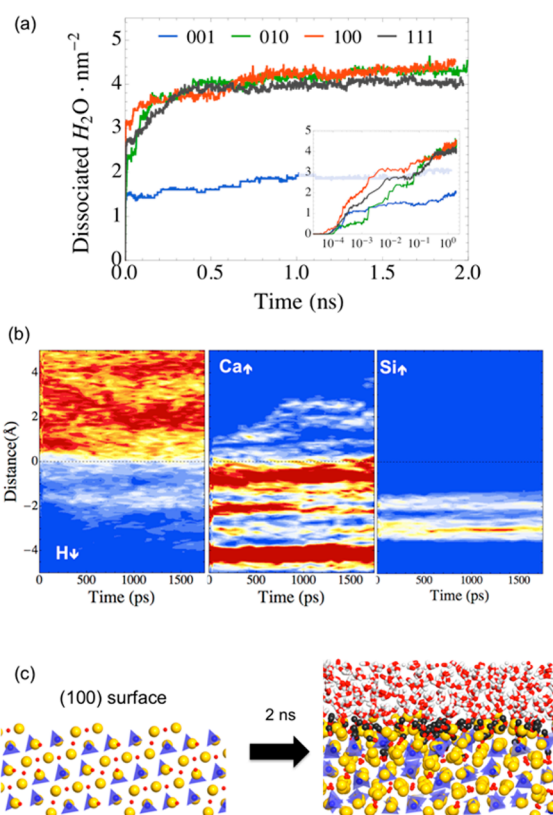

Figure 3. Panel (a) displays the water reacted per surface area for the different surfaces, with logarithmic time scale in the inset to highlight differences at short hydration times. In panel (b.) we present an example of the atomic density profiles of H, Ca, and Si atoms in the direction perpendicular to the (111) surface. The Gibbs plane that defines the boundary between the solid and water has been chosen to match the last atomic plane of the solid, formed by calcium or oxygen atoms depending on the cleavage. The same analysis for all the surfaces is presented in the Supporting Information. Panel (c) shows a snapshot of the same surface before coming into contact with water and after 2 ns of hydration. The hydrogen atoms from dissociated water molecules are represented in black to illustrate their absorption within the mineral structure.

penetrate into the crystal, hopping from one oxygen to another, as reported for proton transfer in perovskites.[42,43]

The amount of adsorbed water into the crystal and its penetration depth can be analyzed by computing the time-resolved atomic density profiles (TRDP). TRDPs specify the density of a given element in the direction perpendicular to the surface, and after defining the position of the Gibbs plane, i.e., the infinitesimal layer that divides the solid and the liquid, they allow us to explore the water adsorption and ion desorption from the solid. In this work, the TRDP were computed using atomic density profiles averaging 5 ps trajectories every 50 ps. We observe a highly variable thickness of the dissolution front, i.e., the space where solid and water species coexist, ranging from 0.3 to 0.8 nm thick depending on the surface. Conversely, as depicted in Figure 3a, the amount of water reacted per surface area unit is almost the same in all the surfaces (4 H_2O nm^{-2}). This result suggests that the crossover in the water dissociation rate is associated with complex structural adjustments and not simply to the saturation of the outermost oxygen atoms. The TRDPs also show the desorption of calcium ions and silicate groups from the solid. Calcium desorbs quickly and tends to accumulate as inner- and outersphere complexes at the
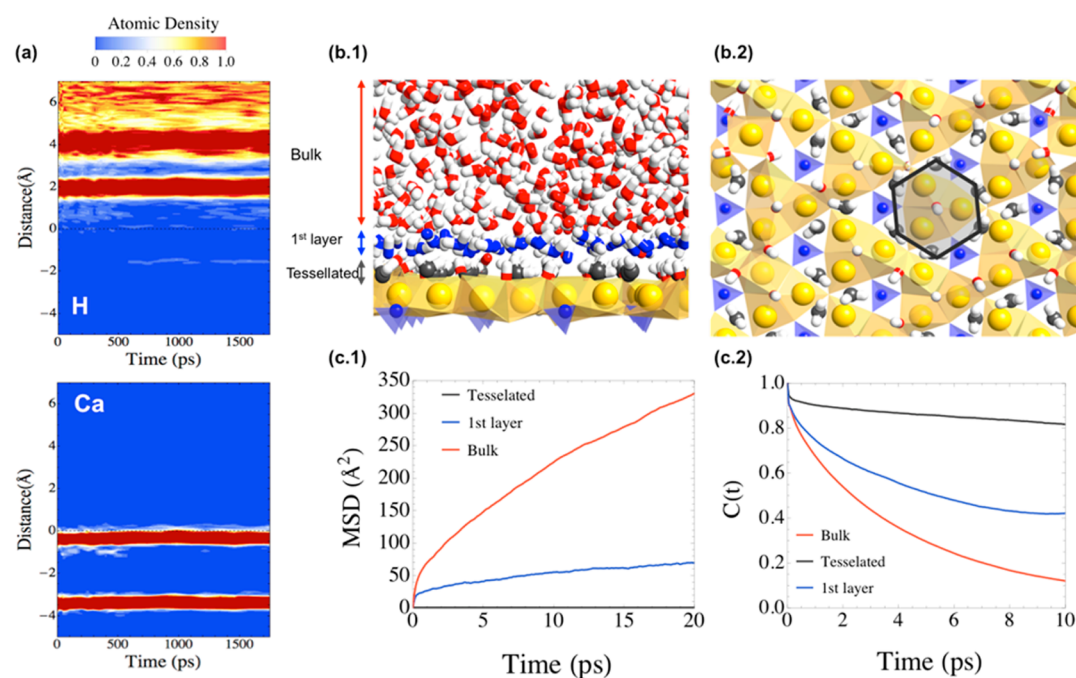
Figure 4. (a) Temporal density profiles of the hydrogen and calcium atoms for the stable (001) surface. The H density profile shows two layers of dense fluid in contact with the surface, which correspond to an icelike half-dissociated monolayer and a first layer of strongly adsorbed water. (b) Representation of those layers, from a snapshot of the MD simulation taken at 1.5 ns. (b.1) In-plane view of the surface where the three water types are noticeable. (b.2) Icelike layer from a top view of the surface. The hexagonal arrangement of the water molecules in the surface can be appreciated. (c.1 and c.2) Dynamics of the water molecules in the three regions. The former displays the dipolar moment autocorrelation function to characterize the rotation, whereas the latter presents the mean square displacement to characterize the translation. Three regimes are evident, each one associated with a type of water in the system.

surface.[7,44−46] The high concentration of metal ions in the surface is also consistent with ζ potential measurements of tricalcium silicate suspensions.[47] Instead, the silicate groups do not translate but rather only rotate with their center of mass held in their initial positions, contributing the formation of a disordered interphase.

Essentially, the dissolution process that we observe is consistent with the ligand-exchange model.[7,44,45] This basic model assumes that the dissolution of an ion from a solid can be viewed as an analogue to a simple ligand-exchange reaction of the ions in solution, in which the exchange is from a metal−oxygen bond of the solid to a metal−oxygen bond of the solvent. In our simulations, we observe that ligand exchange is chemical-reaction-mediated: As water dissociates, hydrogen penetrates into the crystal, protonating oxygen atoms and breaking the calcium bonds with the crystal framework. Ca atoms then desorb toward the solution to fill their coordination shell with water molecules. Therefore, we can state that the ligand exchange is not merely a molecular surface process;[48] therefore, the topochemical reactions occuring as hydrogen migrates into the crystal are key steps of the dissolution. An important technological consequence is that the ligand-exchange model predicts the fastest dissolution rate among orthosilicate minerals to those formed by calcium. Therefore, the reaction rate of tricalcium silicates in cement cannot be increased by cationic substitution (if there are not structural changes or defects associated with it).

Remarkably, as we moved from the static to the dynamic view of dissolution, we found that none of the static surface properties (γ and water adsorption energies) translate into the different hydration rates and mechanisms. The reaction rate is only different at very short reaction times, on the order of tens

of picoseconds as can be seen in Figure 3a (inset). The reason behind the homogeneous behavior of the surfaces is their topological evolution upon hydration. As the reactions proceed, the surfaces lose their crystalline order and form a disordered calcium silicate hydrate. The disorder is originated by the adsorption of water, desorption of calcium, and rearrangement of the silicate tetrahedron. The new interfaces are similar in structure and stoichiometry independent from the initial cleavage, diminishing the impact of different static surface energies on the behavior observed in the hydration process.

Dynamic Picture 2: Water Tesselation. As noted earlier, the water dissociation rate on the (001) surface does not follow the same trend as other surfaces. After initially abrupt water dissociation, the surface becomes stable, and no further reactions are observed. Contrary to the other cases already discussed, for this surface the temporal density profiles do not reveal disorder at the surface. Instead, water molecules organize at the surface without penetrating into the crystal, and calcium ions do not desorb from the surface, maintaining a crystalline order. The cause for this behavior is a water tessellation process, which creates a stable configuration that prevents hydration. Water tessellation, which refers to the patterning of water molecules in a quasi-static 2D sheet, has been observed in various materials,[49−52] and reactive Monte Carlo simulations have shown that it can stabilize crystalline surfaces, inhibiting hydration.[53] In tricalcium silicate, the tessellation takes place by the adsorption of water molecules and hydroxyl groups in well-defined surface sites forming a half-dissociated monolayer with a hexagonal structure. The hydrogen atoms from both water molecules and hydroxyl groups are oriented toward the solution and stabilized by hydrogen bonds with one another as well as with the interfacial bulk water molecules. Similar

arrangements have been found in metal/water interfaces.[49] Interestingly, the presence of hydroxyl groups (half-dissociated monolayer), such as those we find in tricalcium silicate, has been found to be more stable than a molecular monolayer in Ruthenium/water interfaces.[54]

The icelike character of the tessellated water layer is quantified by examining the rotational and translational motion of the molecules. Rotations are characterized by the dipole moment reorientation dynamics. The dipole orientation autocorrelation time ($C(t)$) of water molecules in the tessellated case is similar to that of supercooled water,[55] which indicates a low rotational motion (Figure 4). Further, the mean square displacement of the molecules shows that the water molecules are fixed in their adsorption sites and do not translate. In addition to the well-organized icelike monolayer, we can see from the temporal density profiles that the order extends to the first layer of water molecules, induced by strong interactions with the icelike monolayer. These water molecules display a rotational and translational motion intermediate between that of liquid water and the tessellated water. The decrease or even suppression of translational motion of adsorbed water has been also found by MD simulations in metals[56] and titanium oxide polymorphs.[57] Overall, the surface is stabilized by the formation of a tessellated icelike water layer, a strongly structured water layer with restricted dynamics. These three water regimens were also observed for Rutile and Cassiterite surfaces both from MD simulations and quasi-elastic neutron-scattering experiments.[58]

CONCLUSIONS

Through this work, we have employed reactive force field molecular dynamics to understand the hydration and dissolution of a model orthosilicate mineral, tricalcium silicate. First, we analyzed in depth the static surface energies and the water adsorption energies. To asses properly the relevant quantities, we used a novel procedure to compute the surface energies of asymmetric slabs, and we mapped the water adsorption energy and water dissociation sites in great detail for the whole surface. Interestingly, we did not find any correlation between the investigated static properties.

The lack of correlation becomes even more marked when we move to study the dynamic hydration and dissolution via molecular dynamics simulations of the mineral/water interfaces under realistic conditions. As water reacts with the surface, important topological changes take place modifying the surface structure, and the correlation with the surface properties is lost. Therefore, we conclude that the hydration of minerals cannot be predicted from the static properties as has been traditionally done, and dynamics become necessary to observe the topochemical reactions and understand them.

The hydration mechanism of tricalcium silicate reactive surfaces can be summarized as a reaction and hopping process. Water reacts with the surface oxygen atoms forming hydroxyl pairs. Then, the hydrogen atoms penetrate into the crystal, hopping from surface to inner oxygen atoms following a Grotthuss-type mechanism. The protonation reactions break the calcium–oxygen bonds, and calcium desorbs from the bulk to the surface, forming inner- and outersphere complexes. Overall, the surface of the crystal evolves toward a disordered calcium silicate hydrate. The hydration induces a disorder as the surface evolves toward a hydrated calcium silicate, and as a result, the reaction rates homogenize. However, we also observe an unexpected opposite effect, wherein a water tessellation process preserves the crystalline order of the surface by the formation of a stable icelike monolayer, inhibiting hydration.

ASSOCIATED CONTENT

Ⓢ Supporting Information

Validation of the force field, explanation of the surface energy evaluation method, adsorption energy surfaces (AES) for all the studied surfaces, water chemi- and physisorption configurations, time-resolved atomic density profiles for all the studied surfaces, and example of a proton transfer reaction. The Supporting Information is available free of charge on the ACS Publications website at DOI: 10.1021/acsami.5b02505.

AUTHOR INFORMATION

Corresponding Author
*E-mail: hegoi.manzano@ehu.eus.

Notes
The authors declare no competing financial interest.

REFERENCES

(1) Markewitz, D.; Davidson, E. A.; Figueiredo, Rd; Victoria, R. L.; Krusche, A. V. Control of Cation Concentrations in Stream Waters by Surface Soil Processes in an Amazonian Watershed. *Nature* **2001**, *410*, 802−805.

(2) Mayhew, L. E.; Ellison, E. T.; McCollom, T. M.; Trainor, T. P.; Templeton, A. S. Hydrogen Generation from Low-Temperature Water−rock Reactions. *Nat. Geosci.* **2013**, *6*, 478−484.

(3) Granados, M. L.; Poves, M. D. Z. D. Z.; Alonso, D. M.; Mariscal, R.; Galisteo, F. C.; Moreno-Tost, R.; Santamaría, J.; Fierro, J. L. G. L. G. Biodiesel from Sunflower Oil by Using Activated Calcium Oxide. *Appl. Catal., B* **2007**, *73*, 317−326.

(4) Thomas, J. J.; Biernacki, J. J.; Bullard, J. W.; Bishnoi, S.; Dolado, J. S.; Scherer, G. W.; Luttge, A. Modeling and Simulation of Cement Hydration Kinetics and Microstructure Development. *Cem. Concr. Res.* **2011**, *41*, 1257−1278.

(5) Porter, A. E.; Patel, N.; Skepper, J. N.; Best, S. M.; Bonfield, W. Comparison of in Vivo Dissolution Processes in Hydroxyapatite and Silicon-Substituted Hydroxyapatite Bioceramics. *Biomaterials* **2003**, *24*, 4609−4620.

(6) Lasaga, A. C.; Luttge, A. Variation of Crystal Dissolution Rate Based on a Dissolution Stepwave Model. *Science* **2001**, *291*, 2400−2404.

(7) Stumm, W. Reactivity at the Mineral-Water Interface: Dissolution and Inhibition. *Colloids Surf., A* **1997**, *120*, 143−146.

(8) Liu, G.; Yu, J. C.; Lu, G. Q. (Max); Cheng, H.-M. Crystal Facet Engineering of Semiconductor Photocatalysts: Motivations, Advances and Unique Properties. *Chem. Commun.* **2011**, *47*, 6763−6783.

(9) Cicero, G.; Grossman, J. C.; Catellani, A.; Galli, G. Water at a Hydrophilic Solid Surface Probed by Ab Initio Molecular Dynamics: Inhomogeneous Thin Layers of Dense Fluid. *J. Am. Chem. Soc.* **2005**, *127*, 6830−6835.

(10) Liu, L.; Krack, M.; Michaelides, A. Density Oscillations in a Nanoscale Water Film on Salt: Insight from Ab Initio Molecular Dynamics. *J. Am. Chem. Soc.* **2008**, *130*, 8572−8573.

(11) Minerals Program, U.S. Geological Survey http://minerals.usgs.gov/minerals/pubs/commodity/cement/.

(12) Juilland, P.; Gallucci, E.; Flatt, R.; Scrivener, K. Dissolution Theory Applied to the Induction Period in Alite Hydration. *Cem. Concr. Res.* **2010**, *40*, 831−844.

(13) Van Duin, A. C. T.; Dasgupta, S.; Lorant, F.; Goddard, W. A.; Duin, A. C. T. Van. ReaxFF: A Reactive Force Field for Hydrocarbons. *J. Phys. Chem. A* **2001**, *105*, 9396−9409.

(14) Plimpton, S. Fast Parallel Algorithms for Short-Range Molecular Dynamics. *J. Comput. Phys.* **1995**, *117*, 1−19.

(15) Fogarty, J. C.; Aktulga, H. M.; Grama, A. Y.; van Duin, A. C. T.; Pandit, S. A. A Reactive Molecular Dynamics Simulation of the Silica-Water Interface. *J. Chem. Phys.* **2010**, *132*, 174704.

(16) Manzano, H.; Pellenq, R. J. M.; Ulm, F.-J.; Buehler, M. J.; van Duin, A. C. T. Hydration of Calcium Oxide Surface Predicted by Reactive Force Field Molecular Dynamics. *Langmuir* **2012**, *28*, 4187−4197.

(17) Manzano, H.; Masoero, E.; Lopez-Arbeloa, I.; Jennings, H. M. Shear Deformations in Calcium Silicate Hydrates. *Soft Matter* **2013**, *9*, 7333−7341.

(18) Manzano, H.; Moeini, S.; Marinelli, F.; van Duin, A. C. T.; Ulm, F.-J.; Pellenq, R. J. M. Confined Water Dissociation in Microporous Defective Silicates: Mechanism, Dipole Distribution, and Impact on Substrate Properties. *J. Am. Chem. Soc.* **2012**, *134*, 2208−2215.

(19) Abdolhosseini Qomi, M. J.; Krakowiak, K. J.; Bauchy, M.; Stewart, K. L.; Shahsavari, R.; Jagannathan, D.; Brommer, D. B.; Baronnet, A.; Buehler, M. J.; Yip, S.; Ulm, F.-J.; Van Vliet, K.; Pellenq, R.J-.M. Combinatorial Molecular Optimization of Cement Hydrates. *Nat. Commun.* **2014**, *5*, 4960.

(20) Hou, D.; Zhao, T.; Jin, Z.; Li, Z. Structure, Reactivity and Mechanical Properties of Water Ultra-Confined in the Ordered Crystal: A Case Study of Jennite. *Microporous Mesoporous Mater.* **2015**, *204*, 106−114.

(21) Pitman, M. C.; van Duin, A. C. T. Dynamics of Confined Reactive Water in Smectite Clay/Zeolite Composites. *J. Am. Chem. Soc.* **2012**, *134*, 3042−3053.

(22) Hantal, G.; Brochard, L.; Laubie, H.; Ebrahimi, D.; Pellenq, R. J.-M.; Ulm, F.-J.; Coasne, B. Atomic-Scale Modelling of Elastic and Failure Properties of Clays. *Mol. Phys.* **2014**, *112*, 1294.

(23) Martínez, L.; Andrade, R.; Birgin, E. G.; Martínez, J. M. *PACKMOL: A Package for Building Initial Configurations for Molecular Dynamics Simulations*; Wiley: New York, 2009; Vol. *30*, pp 2157−2164.

(24) Vittadini, A.; Selloni, A.; Rotzinger, F. P.; Grätzel, M. Structure and Energetics of Water Adsorbed at TiO 2 Anatase (101) and (001) Surfaces. *Phys. Rev. Lett.* **1998**, *81*, 2954.

(25) Yang, H. G.; Sun, C. H.; Qiao, S. Z.; Zou, J.; Liu, G.; Smith, S. C.; Cheng, H. M.; Lu, G. Q. Anatase TiO2 Single Crystals with a Large Percentage of Reactive Facets. *Nature* **2008**, *453*, 638−641.

(26) Durgun, E.; Manzano, H.; Pellenq, R. J. M.; Grossman, J. C. Understanding and Controlling the Reactivity of the Calcium Silicate Phases from First Principles. *Chem. Mater.* **2012**, *24*, 1262−1267.

(27) Wang, L.; Zhou, F.; Meng, Y. S.; Ceder, G. First-Principles Study of Surface Properties of LiFePO4: Surface Energy, Structure, Wulff Shape, and Surface Redox Potential. *Phys. Rev. B: Condens. Matter Mater. Phys.* **2007**, *76*, 165435.

(28) Chizallet, C.; Costentin, G.; Che, M.; Delbecq, F.; Sautet, P. Revisiting Acido-Basicity of the MgO Surface by Periodic Density Functional Theory Calculations: Role of Surface Topology and Ion Coordination on Water Dissociation. *J. Phys. Chem. B* **2006**, *110*, 15878−15886.

(29) Durgun, E.; Manzano, H.; Kumar, P. V.; Grossman, J. C. The Characterization, Stability, and Reactivity of Synthetic Calcium Silicate Surfaces from First Principles. *J. Phys. Chem. C* **2014**, *118*, 15214−15219.

(30) Mishra, R. K.; Flatt, R. J.; Heinz, H. Force Field for Tricalcium Silicate and Insight into Nanoscale Properties: Cleavage, Initial Hydration, and Adsorption of Organic Molecules. *J. Phys. Chem. C* **2013**, *117*, 10417−10432.

(31) Recham, N.; Chotard, J.-N.; Dupont, L.; Delacourt, C.; Walker, W.; Armand, M.; Tarascon, J.-M. A 3.6 V Lithium-Based Fluorosulphate Insertion Positive Electrode for Lithium-Ion Batteries. *Nat. Mater.* **2010**, *9*, 68.

(32) Carrasco, J.; Illas, F.; Lopez, N. Dynamic Ion Pairs in the Adsorption of Isolated Water Molecules on Alkaline-Earth Oxide (001) Surfaces. *Phys. Rev. Lett.* **2008**, *100*, 4.

(33) Kerisit, S.; Bylaska, E. J.; Felmy, A. R. Water and Carbon Dioxide Adsorption at Olivine Surfaces. *Chem. Geol.* **2013**, *359*, 81−89.

(34) De Leeuw, N. H. H.; Purton, J. a. A.; Parker, S. C. C.; Watson, G. W. W.; Kresse, G. Density Functional Theory Calculations of Adsorption of Water at Calcium Oxide and Calcium Fluoride Surfaces. *Surf. Sci.* **2000**, *452*, 9−19.

(35) Fernández-Torre, D.; Kośmider, K.; Carrasco, J.; Ganduglia-Pirovano, M. V.; Pérez, R. Insight into the Adsorption of Water on the Clean CeO2(111) Surface with van Der Waals and Hybrid Density Functionals. *J. Phys. Chem. C* **2012**, *116*, 13584−13593.

(36) Raymand, D.; van Duin, A. C. T.; Goddard, W. A.; Hermansson, K.; Spangberg, D. Hydroxylation Structure and Proton Transfer Reactivity at the Zinc Oxide-Water Interface. *J. Phys. Chem. C* **2011**, *115*, 8573−8579.

(37) Guhl, H.; Miller, W.; Reuter, K. Water Adsorption and Dissociation on SrTiO3(001) Revisited: A Density Functional Theory Study. *Phys. Rev. B: Condens. Matter Mater. Phys.* **2010**, *81*, 155455.

(38) de Leeuw, N. H.; Watson, G. W.; Parker, S. C. De. Atomistic Simulation of the Effect of Dissociative Adsorption of Water on the Surface Structure and Stability of Calcium and Magnesium Oxide. *J. Phys. Chem.* **1995**, *99*, 17219−17225.

(39) Manzano, H.; Durgun, E.; Abdolhosseine Qomi, M. J.; Ulm, F.-J.; Pellenq, R. J. M.; Grossman, J. C. Impact of Chemical Impurities on the Crystalline Cement Clinker Phases Determined by Atomistic Simulations. *Cryst. Growth Des.* **2011**, *11*, 2964−2972.

(40) Mahadevan, T. S.; Garofalini, S. H. Dissociative Chemisorption of Water onto Silica Surfaces and Formation of Hydronium Ions. *J. Phys. Chem. C* **2008**, *112*, 1507−1515.

(41) Dunstetter, F.; de Noirfontaine, M. N.; Courtial, M. Polymorphism of Tricalcium Silicate, the Major Compound of Portland Cement Clinker 1. Structural Data: Review and Unified Analysis. *Cem. Concr. Res.* **2006**, *36*, 39−53.

(42) Islam, M. S.; Davies, R. A.; Gale, J. D. Proton Migration and Defect Interactions in the CaZrO3 Orthorhombic Perovskite: A Quantum Mechanical Study. *Chem. Mater.* **2001**, *13*, 2049−2055.

(43) Kreuer, K.-D. Proton Conductivity: Materials and Applications. *Chem. Mater.* **1996**, *8*, 610−641.

(44) Ohlin, C. A.; Villa, E. M.; Rustad, J. R.; Casey, W. H. Dissolution of Insulating Oxide Materials at the Molecular Scale. *Nat. Mater.* **2010**, *9*, 11−19.

(45) Casey, W. H. On the Relative Dissolution Rates of Some Oxide and Orthosilicate Minerals. *J. Colloid Interface Sci.* **1991**, *146*, 586−589.

(46) Thompson, A.; Goyne, K. W. Introduction to the Sorption of Chemical Constituents in Soils. *Nat. Ed. Knowl.* **2012**, *4*, 4−7.

(47) Zingg, A.; Winnefeld, F.; Holzer, L.; Pakusch, J.; Becker, S.; Gauckler, L. Adsorption of Polyelectrolytes and Its Influence on the Rheology, Zeta Potential, and Microstructure of Various Cement and Hydrate Phases. *J. Colloid Interface Sci.* **2008**, *323*, 301−312.

(48) Stack, A. G.; Raiteri, P.; Gale, J. D. Accurate Rates of the Complex Mechanisms for Growth and Dissolution of Minerals Using a Combination of Rare-Event Theories. *J. Am. Chem. Soc.* **2012**, *134*, 11−14.

(49) Carrasco, J.; Hodgson, A.; Michaelides, A. A Molecular Perspective of Water at Metal Interfaces. *Nat. Mater.* **2012**, *11*, 667−674.

(50) Ostroverkhov, V.; Waychunas, G. A.; Shen, Y. R. New Information on Water Interfacial Structure Revealed by Phase-Sensitive Surface Spectroscopy. *Phys. Rev. Lett.* **2005**, *94*, 46102.

(51) Du, Q.; Freysz, E.; Shen, Y. R. Surface Vibrational Spectroscopic Studies of Hydrogen Bonding and Hydrophobicity. *Science* **1994**, *264*, 826−828.

(52) Miranda, P. B.; Xu, L.; Shen, Y. R.; Salmeron, M. Icelike Water Monolayer Adsorbed on Mica at Room Temperature. *Phys. Rev. Lett.* **1998**, *81*, 5876.

(53) Nangia, S.; Garrison, B. J.; Park, U. V.; Pennsyl, V. Role of Intrasurface Hydrogen Bonding on Silica Dissolution. *J. Phys. Chem. C* **2010**, *114*, 2267−2272.

(54) Schnur, S.; Groß, A. Properties of Metal−water Interfaces Studied from First Principles. *New J. Phys.* **2009**, *11*, 125003.

(55) Kumar, P.; Franzese, G.; Buldyrev, S. V.; Stanley, H. E. Molecular Dynamics Study of Orientational Cooperativity in Water. *Phys. Rev. E* **2006**, *73*, 41505.

(56) Limmer, D. T.; Willard, A. P.; Madden, P.; Chandler, D. Hydration of Metal Surfaces Can Be Dynamically Heterogeneous and Hydrophobic. *Proc. Natl. Acad. Sci. U. S. A.* **2013**, *110*, 4200−4205.

(57) Kavathekar, R. S.; English, N. J.; MacElroy, J. M. D. Study of Translational, Librational and Intra-Molecular Motion of Adsorbed Liquid Water Monolayers at Various TiO2 Interfaces. *Mol. Phys.* **2011**, *109*, 2645−2654.

(58) Mamontov, E.; Vlcek, L.; Wesolowski, D. J.; Cummings, P. T.; Wang, W.; Anovitz, L. M.; Rosenqvist, J.; Brown, C. M.; Garcia Sakai, V. Dynamics and Structure of Hydration Water on Rutile and Cassiterite Nanopowders Studied by Quasielastic Neutron Scattering and Molecular Dynamics Simulations. *J. Phys. Chem. C* **2007**, *111*, 4328−4341.